

Polarimetric optical fiber sensors of a new generation for industrial applications

T.R. WOLIŃSKI*, P. LESIAK, and A.W. DOMAŃSKI

Faculty of Physics, Warsaw University of Technology,
 75 Koszykowa St., 00-662 Warszawa, Poland

Abstract. Polarimetric optical fiber sensors based on highly birefringent (HB) polarization-maintaining fibers have focused great interest for last decades. The paper presents a novel modular fiber optic sensing system of potential industrial applications to measure temperature, hydrostatic pressure, and strain that is based on classical HB and photonic crystal fibers and can operate at visible and infrared wavelengths. The main idea of the system is a novel and replaceable fiber-optic head, which allows adjusting the measuring system both to the required range and type (strain, pressure or temperature) of the external measurand. We propose also a new configuration of the fiber optic strain gauge with a free cylinder and an all-fiber built-in analyzer based on the photonic crystal fiber filled with a liquid crystal. Additionally, strain sensitivities of various HB fibers operating at visible and infrared wavelengths range have been measured.

Key words: highly birefringent fibers, polarimetric fiber sensors, photonic (liquid) crystal fibers.

1. Introduction

Polarimetric optical fiber sensors based on highly birefringent (HB) polarization-maintaining fibers have focused great interest for last decades [1–5]. In HB fibers, the difference between the phase velocities for the two orthogonally polarized modes is high enough to avoid coupling between these two modes. Fibers of this class have a built-in, well-defined, high internal birefringence obtained by designing a core and/or cladding with noncircular (mostly elliptical) geometry, or by using anisotropic stress applying parts built into the cross-section of the fiber.

The modal behavior of the lowest-order mode HB fibers under various external deformations is of special interest for sensors and device applications. A number of physical quantities can be measured on the basis of HB fibers: hydrostatic pressure, strain, vibration, temperature, acoustic wave, etc.

A symmetric deformation effect (X) influences the propagation constant β in every mode because of the changes in fiber length L and the refractive indices of the core and the cladding. In a single-mode regime, this leads to changes in the phase difference $\Delta\Phi = \Delta\beta \cdot L$ between both polarizations of the fundamental LP_{01} mode along the fiber [1]:

$$\frac{\delta(\Delta\Phi)}{\delta X} = \Delta\beta \frac{\partial L}{\partial X} + L \frac{\partial(\Delta\beta)}{\partial X} \quad (1)$$

where X stands for temperature (T), pressure (p) or longitudinal strain (ε) defined as: $\varepsilon = \Delta L/L$.

The effect of longitudinal strain on mode coupling is to modulate the relative phase retardation between the two orthogonal polarizations in the LP_{01} mode. The general formula describing the birefringence sensitivity to strain can be expressed in terms of an experimental parameter T_ε describing

the amount of strain ε required to induce a 2π phase shift of a polarized light observed at the output as [3]:

$$\Delta\beta(\varepsilon) = \Delta\beta^0 + \operatorname{sgn} \left[\frac{d(\Delta\beta)}{d\varepsilon} \right] \varepsilon \frac{2\pi}{T_\varepsilon L} \quad (2)$$

where $\Delta\beta_L^0$ signifies unperturbed modal (polarization) birefringence of a fiber and the function $\operatorname{sgn} \left[\frac{d(\Delta\beta)}{d\varepsilon} \right]$ has two values: $+1$ or -1 depending on the sign of the changes in the relative polarization birefringence with strain and L is the total optical path of the fiber.

Under influence of the longitudinal strain the first term on the right-hand side of expression (1) is negligible with respect to the first, so that:

$$\delta(\Delta\Phi) \cong \frac{\partial(\Delta\beta)}{\partial\varepsilon} L\varepsilon = \frac{\partial(\Delta\beta)}{\partial\varepsilon} \delta L \quad (3)$$

Hence the phase changes of the polarimetric responses are proportional to the absolute elongation ΔL and are independent of the length L of the sensing region. Under the influence of a longitudinal axial strain, the equation (3) can be approximated with the use of formulae (2) in terms of the only experimental parameter T_ε

$$\frac{\delta(\Delta\Phi_i)}{\delta\varepsilon} = \Delta\beta_i \frac{\partial L}{\partial\varepsilon} + \operatorname{sgn} \frac{d(\Delta\beta_i)}{d\varepsilon} \cdot \frac{2\pi}{T_\varepsilon^i} \cong \operatorname{sgn} \frac{d(\Delta\beta_i)}{d\varepsilon} \cdot \frac{2\pi}{T_\varepsilon^i} \quad (4)$$

Based on the formula (4) we can calculate strain sensitivity (S) of the HB fiber section of the length L as follows:

$$S = \frac{2\pi}{T_\varepsilon \cdot L} \quad [\text{rad}/(\text{m}\varepsilon \cdot \text{m})] \quad (5)$$

*e-mail: wolinski@if.pw.edu.pl

The value of the parameter T_ϵ multiplied by length of the fiber L is a wavelength-dependent constant:

$$L \cdot T_\epsilon = \text{const}(\lambda) \quad (6)$$

and this dependence originally established for HB *bow-tie* fibers [4] enables a variety of possibilities to construct fiber-optic strain gauges precisely adjusted to particular applications.

2. Materials and measurement systems

Polarimetric measurements have been performed for different types of HB fibers (see Fig. 1) and for selected wavelengths ranges: around 600 nm, around 800 nm and in the range 1270–1640 nm. In the experimental we measured commercially available HB *bow-tie* fibers (HB 600, HB 800 and HB 1500) from Fibercore (UK) and HB PANDA fibers produced either by Fiberlogix (1500) or by Nufern (1300 and 1500); all of them operating in a single-mode regime.

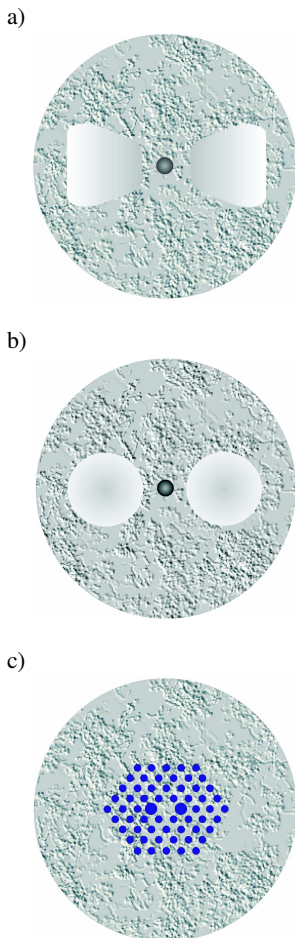


Fig. 1. Types of the HB fibers: (a) *bow-tie*, (b) PANDA, (c) photonic crystal fiber

The measurement setup (Fig. 2) included the Tunics PLUS tunable laser source (TLS) operating within the wavelength range 1500–1640 nm and coupled to the polarimeter PAT 9000B that detected the output state of polarization and served also as a power meter.

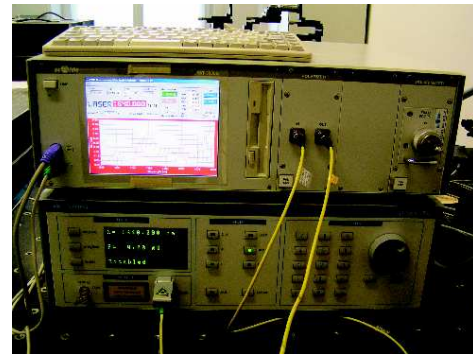


Fig. 2. Strain sensitivity measurement system for the wavelength range up to 1640 nm

The measurement setup for visible and near-infrared wavelengths included different types of the laser sources: a He-Ne laser, various semiconductor laser diodes and a superluminescent diode (SLD).

Additional measurements at infrared (1270–1620 nm) were performed at Vrije Universiteit Brussel (VUB) by using the Santec TLS operating within the wavelength ranges 1270–1340 nm, 1450–1530 nm and 1520–1620 nm operating with the polarimeter HP that detected the output state of polarization and served as a power meter. Multiparameter measurement system (shown in the Fig. 3) was used to characterize the PANDA fiber made by FiberLogix.

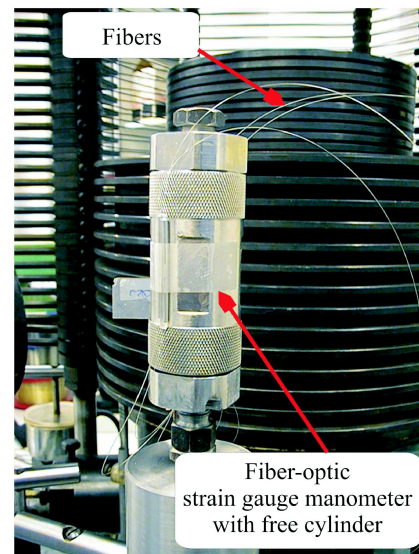


Fig. 3. Free-cylinder strain-gauge pressure transducer

Figure 3 shows the free-cylinder strain-gauge pressure transducer which can be used for pressure measurements in liquid media up to 0.5 GPa [5]. The active cylinder – located inside two cups – is of the hexagonal shape in its central part. It was designed in order to reduce mechanical friction with the cups when pressure is applied. On surface of the hexagonal prism classical 350-Ohm strain gauges are longitudinally and circumferentially bonded in order to detect strains. Pressure is applied to this cylinder both internally and at its ends.

3. Strain sensitivity

It is well known that strain sensitivity depends on wavelength [6–9]. Our measurements indicate that for shorter wavelengths HB fibers are characterized by high strain sensitivities in comparison to telecommunication wavelengths (Fig. 4 and Tab. 1). Strain sensitivities were calculated according to the formula (5).

Figure 4 illustrates influence of the wavelength on longitudinal strain sensitivity. The upper x axis represents visible wavelength range and it is designed for HB 600 and HB 800 *bow-tie* fibers measurements results. The lower x axis represents a telecommunication wavelength range and it is designed

for the HB PANDA fiber measurements results. In single-mode HB fibers (HB-600 and HB-800 *bow-tie* fibers) spectral dependence of strain sensitivity has a nonlinear character. Small wavelength changes induce large changes in longitudinal strain sensitivity. For telecommunication wavelengths (HB PANDA fiber) strain sensitivity also depends on wavelength but in this case this dependence has linear character. Besides, it is a slowly-varying linear function of wavelength. As it results from Fig. 4. strain sensitivities of both HB 600 and HB 800 *bow-tie* fibers at visible wavelengths are larger (about twice) than strain sensitivity of the HB 1500 *bow-tie* fiber at infrared.

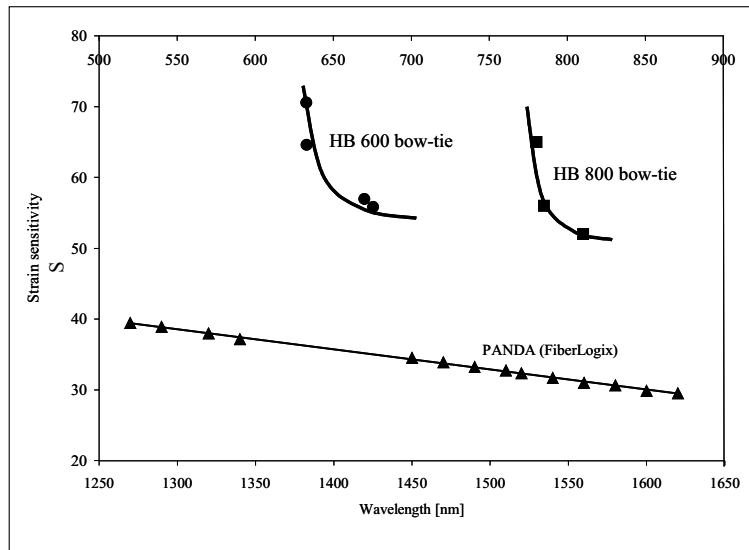


Fig. 4. Comparison between longitudinal strain sensitivity S [rad/(mε· m)] dependences on the wavelength for different HB fibers

Table 1
Comparison between longitudinal strain sensitivity S [rad/(mε· m)] measured in different HB standard fibers;
* after Ref. [10], ** after Ref. [11], *** after Ref. [12]

λ	HB <i>bow-tie</i>	PANDA Nufern	PANDA FiberLogix
600 nm	70*		
800 nm	65**		
1550 nm	32***	34.5	28

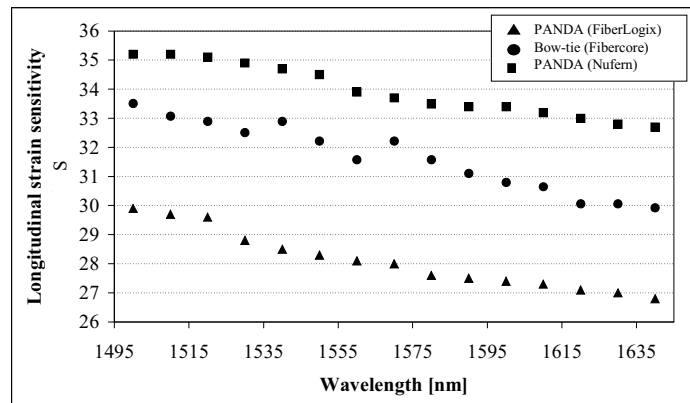


Fig. 5. Comparison between longitudinal strain sensitivity S [rad/(mε· m)] dependences on the wavelength for different HB fibers

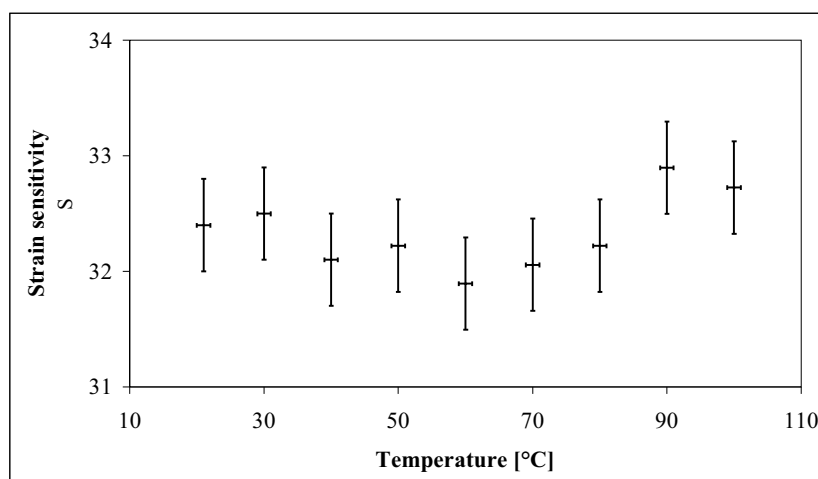


Fig. 6. Longitudinal strain sensitivity S [rad/(m ϵ · m)] vs. temperature measured at 1550 nm

Measurements of strain sensitivities for different types of the HB fibers at 1500–1640 nm wavelengths range were performed on the measurement system shown in Fig. 2. Figure 5 compares strain sensitivities of the HB PANDA fibers made by Nufern and FiberLogix with the HB 1500 *bow-tie* fiber made by Fibercore. The PANDA fiber made by Nufern exhibits the highest strain sensitivity. Spectral dependence of the strain sensitivity in measured HB fibers has a similar character.

Few measurements for different light sources at the same wavelength confirm that the longitudinal strain sensitivity is independent on the laser bandwidth [9]. Strain sensitivity of the HB PANDA fiber was measured by using four different light sources: the Tunic Plus TLS with bandwidth equal to 0.2 pm, the Santec TLS with bandwidth equal to 18 pm, a superluminescence diode with bandwidth equal to 80 nm, and an amplified spontaneous emission (ASE) source with bandwidth equal to 100 nm. All these measurements included the 1520–1620 nm wavelength range. Measurements for tunable laser sources were performed separately with the 10 nm step. Longitudinal strain sensitivities near 1600 nm were close to 28 rad/(m ϵ · m) in each fiber.

Measurements performed at different temperatures at the same wavelength confirm that the longitudinal strain sensitivity is independent on temperature. Strain sensitivity of the HB 1500 *bow-tie* fiber was measured by using a tunable laser source at 1550 nm at selected temperatures from the range 20–100°C (Fig. 6). The output state of polarization of the light coming out of the HB *bow-tie* fiber strongly depends on temperature as well as on longitudinal strain and in consequence it is difficult to distinguish both effects.

4. Fiber optic strain gauge

In 1993 a fiber-optic strain-gauge manometer up to 100 MPa was proposed and patented [13]. The main element of this construction was based on the strain-gauge free-cylinder pressure transducer. An active element of the transducer was composed of the attached HB fiber serving as a strain sensor (Fig. 7).

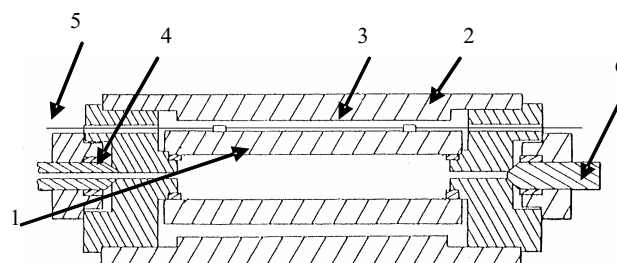


Fig. 7. Fiber-optic strain gauge manometer with free cylinder: 1 – free dilating cylinder; 2 – external protective cover; 3 – strain-sensitive optical fiber; 4 – pressure inlet; 5 – input/output optical fiber; 6 – closing element

This sensor was characterized by relative the phase retardation between two perpendicular eigenmodes influenced by pressure according to the equation:

$$\frac{d\Delta\Phi}{dp} = -\frac{\pi\nu D}{dE\lambda} L \frac{d\Delta n}{dp} \quad (7)$$

where E is the Young modulus, ν is the Poisson ratio, d is the thickness of the cylinder, D is the inner diameter of the cylinder.

In this paper we propose another configuration of the fiber optic strain gauge with a free cylinder presented in Fig. 8. Here, the HB fiber is wounded clockwise on the pressure transducer. Hydrostatic pressure causes modifications of the transducer dimensions and hence induces additional birefringence in the HB fiber due to bend deformation. The induced birefringence influences light polarization at the output of the HB fiber. This instrument allows for measurement of strain induced by hydrostatic pressure according to the dependence:

$$\varepsilon(p) = \frac{p}{E} \frac{2}{K^2 - 1} \quad (8)$$

where E is the Young modulus and K is a parameter of the transducer.

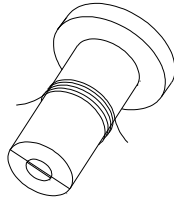


Fig. 8. Fiber optic strain gauge with a free cylinder

In polarimetric optical fiber sensors light intensity at the output is described by the following formulae:

$$I = \frac{1}{2} [1 + \cos(\Delta\Phi)] \quad (9)$$

Based on the formula (1), (2), (8) and (9) we can calculate the output light intensity of the pressure sensor as follows:

$$I = \frac{1}{2} \left\{ 1 + \cos \left[\left(\Delta\beta_i^0 + \operatorname{sgn} \left(\frac{d\Delta\beta_i}{d\varepsilon} \right) \frac{2\pi p}{LT_i^\varepsilon E K^2 - 1} \right) L \right] \right\} \quad (10)$$

In the experimental we used a commercially available HB-800 *bow-tie* fiber manufactured by Fibercore (UK).

Figure 9 shows an optical instrumentation system designed to deliver an input light of the controlled polarization to the sensing section and to detect a pressure-modulated output signal of the sensing element. A linearly polarized light was lunched from a laser emitting diode at 785 nm into the input

HB-800 *bow-tie* fiber. To precisely align the polarization plane of the light parallel to one of two principal birefringence axes, an operating system including a quarter-wave plate and a polarizer was used. To avoid any influences of environmental parameters on light propagation in the sensor element, input and output HB fibers were spliced at 45° (or alternatively connected by FC/PC connectors at 45°) to the HB sensing fiber. Then the light signal is lead by the output fiber to an analyzer and a detector.

The fiber-optic pressure sensor with a temperature compensation system – two sections of the HB-800 fiber with identical lengths spliced with birefringence axes rotated at 90° to each other [14] – has been characterized for pressures in the range from 100 MPa to 300 MPa. Figure 10 shows pressure characteristics of the sensor element 0.125 m long, whereas Fig. 11 shows pressure characteristics of sensor element having 0.6 m in the length. The solid lines are theoretically calculated according to the formulae (10).

Figures 10 and 11 show pressure characteristics of the sensors that use different lengths of the sensing elements to be easily adjusted to different ranges of the measured pressure. For the sensor with 0.125 m in the length of the sensing element, its sensing range is over 200 MPa. For 0.6 m length of sensing element, the sensor is working in the range of ~40 MPa but with a significantly higher resolution. The parameter $T\varepsilon$ in the first case is equal to 400 MPa, whereas in the second 80 MPa. Therefore, a good agreement with the formulae (4) was obtained.

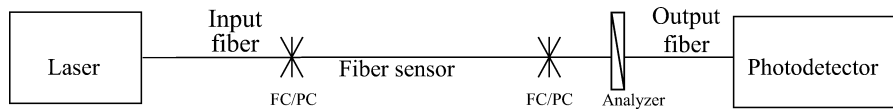


Fig. 9. Optical instrumentation of the optical fiber pressure sensor based on the standard HB fibers

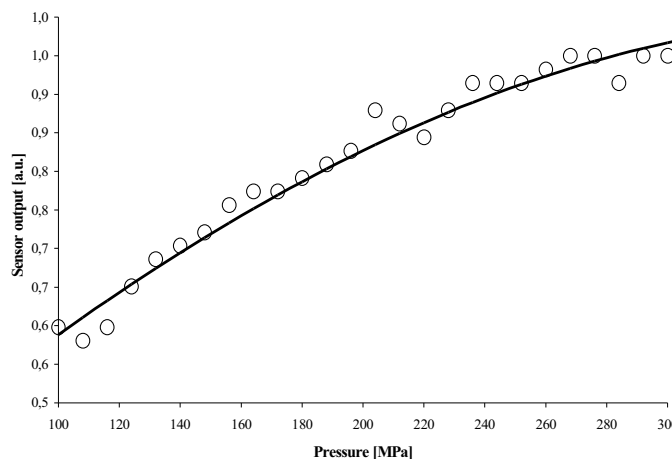


Fig. 10. Characteristics of the fiber-optic pressure sensor with the HB-800 fiber sensing element 0.125 m long

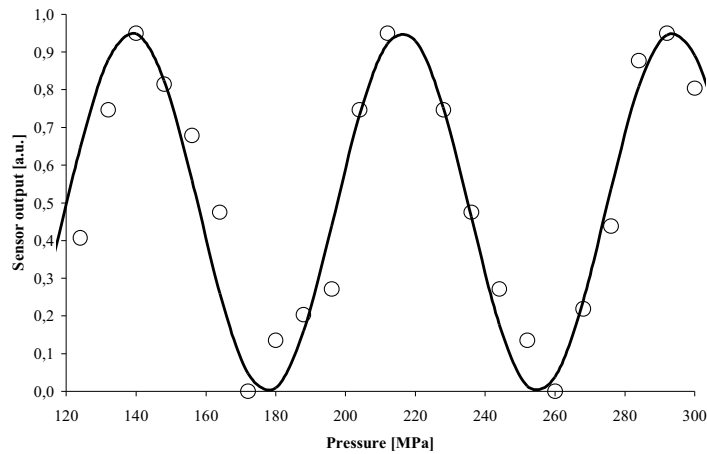


Fig. 11. Characteristics of the fiber pressure sensor with the HB-800 fiber sensing element 0.6 m long

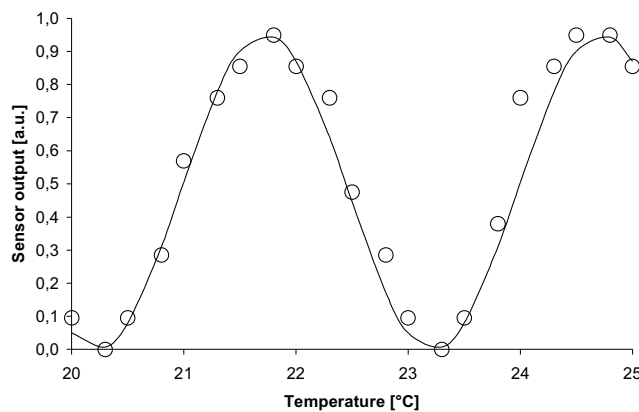


Fig. 12. Characteristics of the temperature sensor based on the HB 800 fiber, 0.6 m long

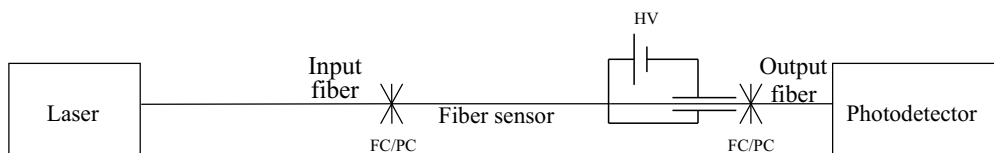


Fig. 13. Optical instrumentation of the optical fiber pressure sensor based on the PCF fibers with the PLCF as the analyzer

The fiber-optic temperature sensor has been characterized at a constant pressure for temperatures in the range from 20°C to 80°C. Figure 12 shows temperature characteristics of the sensor element having 0.6 m in the length in a short range of temperature (20°C ÷ 25°C). A solid line is a theoretical line described by the dependence (3).

Figure 13 shows an optical instrumentation system designed to deliver a linearly polarized input light to the sensing section and to detect a pressure-modulated output signal of the sensing element. A linearly polarized light was launched from a laser emitting diode at 1550 nm into the input HB 1550-01 photonic crystal fiber (PCF) parallel to one of two principal birefringence axes. To avoid any influences of environmental

parameters on light propagation in the sensor element, both input and output HB fibers were connected by FC/PC connectors at 45° to the HB sensing fiber. As an analyzer the photonic liquid crystal fiber (PLCF) was used [15].

A non-circular core combined with the large air-glass refractive index step in photonic crystal fiber creates strong form birefringence. This fiber was used as a host structure, while LCs played a role of guest materials. In the PM-1550-01 HB PCF only two large holes were filled with a liquid crystal (Fig. 14).

As a guest material we used nematic highly birefringence LC mixture cat. no. 1294 1B manufactured at Military University of Technology in Warsaw [15–17].

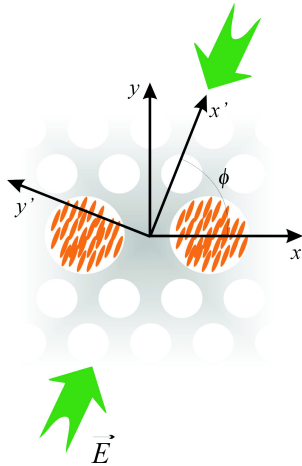


Fig. 14. PLCF (based on the HB 550-01 PCF) under external a.c. electric field

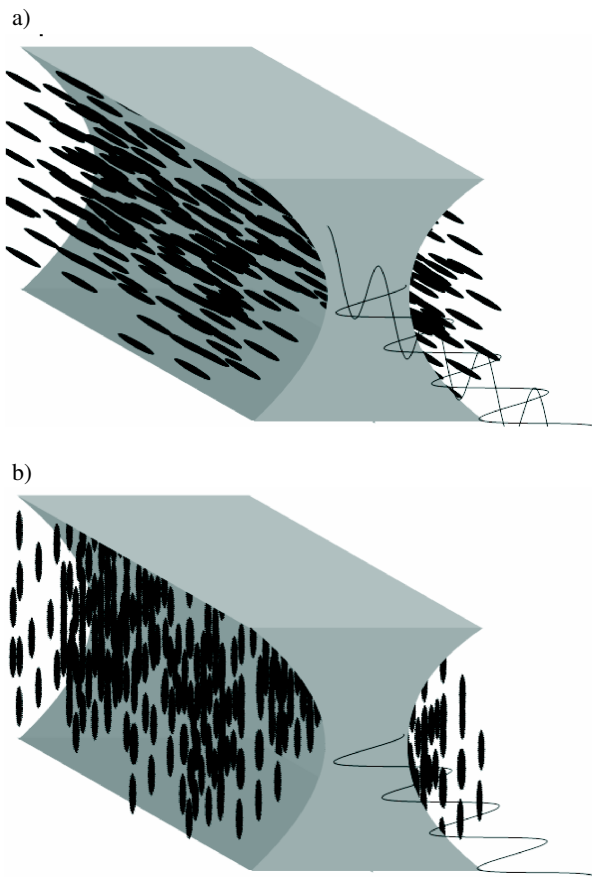


Fig. 15. PLCF used as an analyzer: (a) at $0 \text{ V}/\mu\text{m}$ – planar alignment of the LC molecules enables propagation of both polarizations; (b) at $2.8 \text{ V}/\mu\text{m}$ – LC molecules are reoriented and only one polarization is propagated

As it was presented elsewhere [17] a PLCF in the presence of an external electrical field acts as a single polarization fiber. In the off-voltage state the PLCF was almost insensitive to polarization (see Fig. 15a). This behavior results generally from the fact that the planar alignment of the molecules in the

holes was obtained. In the high-voltage state (Fig. 15b), the PLCF becomes highly sensitive to the input linear polarization due to reorientation of the LC molecules that induce high anisotropy of the PLCF cross-section. Consequently, a significant modulation of the detected output intensity in function of the input polarization can be observed [17].

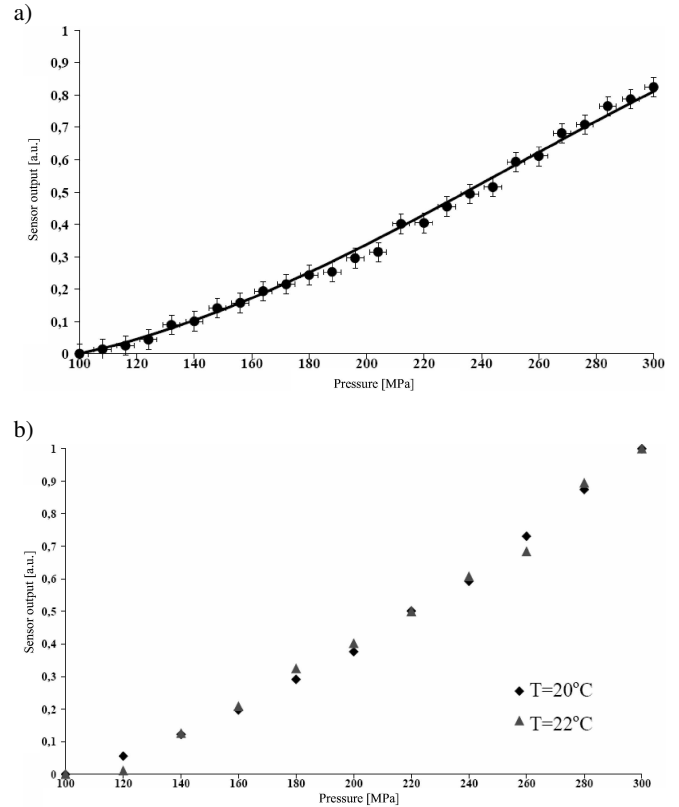


Fig. 16. Pressure characteristics of the fiber-optic sensor with the HB 1550-01 PCF sensing element 0.65 m long (a); along with its thermal stability (b)

The fiber-optic pressure sensor has been characterized for pressures in the range from 100 MPa to 300 MPa. Figure 16a shows pressure characteristics of the sensor element 0.65 m long. The solid line is theoretically calculated according to the formulae (8). Additionally the thermal stability of the pressure sensor was measured (see Fig. 16b). Moreover, long-term stability of the obtained results received within several days was confirmed.

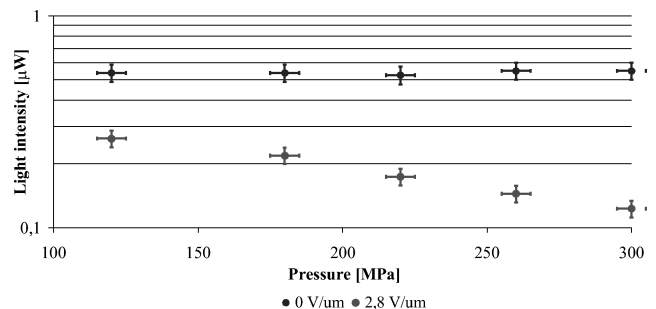


Fig. 17. Influence of the external electrical field on the output signal of the sensor

Figure 17 demonstrates influence of the external electrical field on the characteristics of the pressure sensor. In the off-voltage state the PLCF output light intensity was almost insensitive to pressure but in the high-voltage state, the output signal strongly depended on pressure.

5. Conclusions

In this work temperature and wavelength influences on the longitudinal strain sensitivity in highly birefringent fibers have been investigated. Measurements of the strain sensitivity for different light sources enabled us to investigate impact of both the operating wavelength and the light source bandwidth on polarimetric fiber-optic sensor characteristics. Different light sources operating at the same wavelengths prove that longitudinal strain sensitivity is independent on the source bandwidth. Additional measurements for different temperatures confirm that the longitudinal strain sensitivity is temperature independent.

It appeared that for telecommunication wavelengths (close to the third low-attenuation window) the strain sensitivity is a slowly-varying linear function of wavelength while at visible wavelengths it is strongly wavelength-dependent and has a nonlinear character.

Additionally, a modular fiber optic sensing system with a photonic liquid crystal fiber (acting as an analyzer) for temperature, hydrostatic pressure and/or strain measurements operating at infrared wavelengths was presented. The main idea of the system relies on a new replaceable fiber-optic head (connected to the system by FC/PC connectors), which allows adjusting the measuring system to both a required range and a type (strain, pressure or temperature) of the external measurand.

The presented results create new opportunities for industrial applications of the polarimetric optical fiber sensors discussed in this paper.

Acknowledgements. This paper was supported by the Polish Ministry of Science and Higher Education under the grant no PBZ-MIN-009/T11/2003 and also partially by the European Network of Excellence on Micro-Optics (NEMO).

REFERENCES

- [1] T.R. Woliński, "Polarimetric optical fibers and sensors", in *Progress in Optics*, ed. Emil Wolf, vol. XL, pp. 1–75, Amsterdam, 2000.
- [2] T.R. Woliński, "Polarization phenomena in optical systems", in *Enc. Opt. Engineering*, ed. R. Diggers, M. Dekker, pp. 2150–2175, New York, 2003.
- [3] W.J. Bock, A.W. Domański, and T.R. Woliński, "Influence of high hydrostatic pressure on beat length in highly birefringent single-mode bow-tie fibers", *Appl. Optics* 29, 3484–3488 (1990).
- [4] W.J. Bock, T.R. Woliński, and T. Eftimov, "Polarimetric fibre-optic strain gauge using two-mode highly birefringent fibres", *Pure and Applied Optics: J. Europ. Optical Society* 5, 125–139 (1996).
- [5] P. Lesiak, T.R. Woliński, J. Tul, A.W. Domański, and R. Wiśniewski, "A new fiber optic modular sensing system for pressure, strain, and temperature measurements", *Proc. SPIE* 6188, 61881A (2006).
- [6] W. Urbańczyk, T. Martynkien, and W.J. Bock, "Dispersion effects in elliptical core highly birefringent fibers", *Appl. Optics* 40 (12), 1911–1920 (2001).
- [7] T. Nasiłowski, P. Lesiak, R. Kotyński, M.K. Antkowiak, F. Berghmans, P. Mergo, J. Wójcik, and H. Thienpont, "Multi-parameter sensitivities of birefringent photonic crystal fiber", *Proc. SPIE* 5576, 68–73 (2004).
- [8] J.N. Blake, S.Y. Huang, and B.Y. Kim, and H.J. Shaw, "Strain effect on highly elliptical core two-mode fibers," *Opt. Lett.* 12, 732–734 (1997).
- [9] T.R. Woliński, P. Lesiak, M. Koźlik, A.W. Domański, T. Nasiłowski, and H. Thienpont, "Thermal and spectral effects in polarimetric strain sensors based on highly birefringent fibers", *Proc. SPIE* 5952, 59520K (2005).
- [10] F. Zhang and J. W.Y. Lit, "Temperature and strain sensitivity measurements of high birefringent polarization maintaining fibers", *Applied Optics* 32, 2213–2218 (1993).
- [11] S. Y. Huang, J.N. Blake, and B.Y. Kim, "Perturbation effects on mode propagation in highly elliptical core two-mode fibers", *J. Lightwave Technology* 8, 23–33 (1990).
- [12] T.R. Woliński, P. Lesiak, K. Szaniawska, A.W. Domański, and J. Wójcik, "Polarization mode dispersion in birefringent microstructured fibers", *Optica Applicata* 34, 541–549 (2004).
- [13] W.J. Bock, T.R. Woliński, and R. Wiśniewski, "Fiber-optic strain gauge manometer", *US Patent, No. 5 187 983*, issued on February 23, 1993.
- [14] W.J. Bock and T.R. Woliński, "Temperature-compensated strain sensor based on polarization-rotated reflection", *Fiber Optic Smart Structures and Skins III, Proc. SPIE* 1370, 189–196 (1990).
- [15] S. Ertman, T.R. Woliński, K. Szaniawska, P. Lesiak, A.W. Domański, R. Dąbrowski, E. Nowinowski-Kruszelnicki, and J. Wójcik, "Influence of electrical field on light propagation in microstructured liquid crystal fibers", *Proc. SPIE* 5950, 326–332 (2005).
- [16] T.R. Woliński, K. Szaniawska, S. Ertman, P. Lesiak, A.W. Domański, R. Dąbrowski, E. Nowinowski-Kruszelnicki, and J. Wójcik, "Spectral and polarization properties of microstructured liquid crystal fibers", *Proc. SPIE* 5936, 169–176 (2005).
- [17] P. Lesiak, T.R. Woliński, J. Tul, and A.W. Domański, "All fiber optic modular sensing system for hydrostatic pressure measurements with a photonic liquid crystal fiber analyzer", *Proc. SPIE* 6608, 66081K (2007).